J|A|C|S ARTICLES

Published on Web 04/20/2009

Monitoring Supported-Nanocluster Heterogeneous Catalyst Formation: Product and Kinetic Evidence for a 2-Step, Nucleation and Autocatalytic Growth Mechanism of $Pt(0)_n$ Formation from H_2PtCl_6 on Al_2O_3 or TiO_2

Joseph E. Mondloch, Xinhuan Yan, and Richard G. Finke*

Department of Chemistry, Colorado State University, Fort Collins, Colorado 80523

Received November 15, 2008; E-mail: rfinke@lamar.colostate.edu

Abstract: A pressing problem in supported-metal-nanoparticle heterogeneous catalysis—despite the long history and considerable fundamental as well as industrial importance of such heterogeneous catalysts—is how to monitor such catalysts' formation more routinely, rapidly, and in real time. Such information is needed to better control the size, shape, composition, and thus resultant catalytic activity, selectivity, and lifetime of these important catalysts. To this end, a study is reported of the formation of supported $Pt(0)_n$ nanoparticles by H_2 reduction of H_2PtCl_6 on Al_2O_3 (or TiO_2) to give 6 equivalents of HCl plus supported $Pt(0)_n/Al_2O_3$ (or $Pt(0)_n/TiO_2$), all while in contact with a solution of EtOH and cyclohexene. The HCl and $Pt(0)_n$ products were confirmed, respectively, by the stoichiometry of HCl formation using $pH_{apparent}$ measurements, appropriate standards, and by TEM and EDX measurements. The hypothesis of this research is that the kinetics of formation of this supported heterogeneous catalyst could be successfully monitored by a fast cyclohexene hydrogenation catalytic reporter reaction method first worked out for monitoring transition-metal nanoparticle formation in solution (Watzky, M. A.; Finke, R. G. *J. Am. Chem. Soc.* **1997**, *119*, 10382−10400). Significantly, sigmoidal kinetics of $Pt(0)_n/Al_2O_3$ catalyst formation were in fact successfully monitored by the catalytic hydrogenation reporter reaction method and then found to be well fit to the Finke–Watzky (hereafter F−W) 2-step, slow continuous nucleation and then autocatalytic surface growth mechanism, $A \rightarrow B$ (rate constant k_1) and $A + B \rightarrow 2B$ (rate constant k_2), respectively, in which A is the H_2PtCl_6 and B is the growing, catalytically active Pt(0) nanoparticle surface. The finding that the F−W mechanism is applicable is significant in that it, in turn, suggests that the ≥8 insights from studies of the mechanisms of soluble nanocluster formation can likely also be applied to supported heterogeneous catalyst synthesis, including a recent equation that gives nanocluster size vs time in terms of k_1, k_2, $[A]_o$ and other parameters (Watzky, M. A.; Finney, E. E.; Finke, R. G. *J. Am. Chem. Soc.* **2008**, *130*, 11959−11969). Also presented are the use of the catalytic reporter reaction to reveal H_2 gas to-solution mass-transfer-limitations (MTL) in the system of H_2PtCl_6 on TiO_2, results relevant to a recent communication in this journal. The use of the F−W 2-step nucleation and autocatalytic growth kinetic model to fit 3 literature examples of heterogeneous catalyst formation, involving H_2 reduction of both supported or bulk M_xO_y (i.e., and in gas−solid reactions), are also presented as part of the Supporting Information. A conclusion section is then provided summarizing the insights and caveats from the present work, as well as some needed future studies.

Introduction

Heterogeneous catalysts—often in the form of finely dispersed metal nanoclusters supported on inert materials[1]—are used in many important industrial catalytic processes.[2] However and despite the extensive literature on heterogeneous catalyst preparation,[3] relatively little is known about the mechanism of formation of the active catalyst.[4] One main reason for this paucity of mechanistic information is the lack of experimental methods able to follow heterogeneous catalyst formation in real time.[4] Early studies in the 1970s and 1980s focused on the formation of nanoclusters in zeolites using primarily H_2 uptake

(1) Gates, B. C. *Catalytic Chemistry*; John Wiley & Sons: New York, 1992.

(2) (a) Heinemann, H. Development of Industrial Catalysis. In *Handbook of Heterogeneous Catalysis*; Ertl, G., Knözinger, H., Weitkamp, J., Eds.; VCH: Weinham, 1997; Vol. 1, pp 35−38. (b) Bartholomew, C. H.; Farrauto, R. J. *Fundamentals of Industrial Catalytic Processes*, 2nd ed.; John Wiley & Sons: Hoboken, 2006.

(3) *Preparation of Solid Catalysts*; Ertl, G., Knözinger, J., Weitkamp, J., Eds.; Wiley-VCH: Weinheim, 1999. (a) *Catalyst Preparation Science and Engineering*; Regalbuto, J., Ed.; CRC Press: Boca Raton, FL, 2007.

(4) (a) Lambert, J.-F.; Che, M. *J. Mol. Catal. A: Chem.* **2000**, *162*, 5–18. (b) Oudenhuijzen, M. K.; Kooyman, P. J.; Tappel, B.; van Bokhoven, J. A.; Koningsberger, D. C. *J. Catal.* **2002**, *205*, 135–146. (c) Chupas, P. J.; Chapman, K. W.; Jennings, G.; Lee, P. L.; Grey, C. P. *J. Am. Chem. Soc.* **2007**, *129*, 13822–13824.

(5) (a) Herd, A. C.; Pope, C. G. *J. Chem. Soc. Faraday Trans* **1973**, *69*, 833–838. (b) Kermarec, M.; Briend-Faure, M.; Delafosse, D. *J. Chem. Soc. Chem. Comm.* **1975**, *8*, 272–273. (c) Beyer, H.; Jacobs, P. A.; Uytterhoeven, J. B. *J. Chem. Soc. Faraday Trans* **1976**, *72*, 674–685. (d) Jacobs, P. A.; Tielen, M.; Linart, J.-P.; Uytterhoeven, J. B.; Beyer, H. *J. Chem. Soc. Faraday Trans* **1976**, *72*, 2793–2804.

 © 2009 American Chemical Society

data to obtain kinetics.[5] More recent studies have examined particle formation on both SiO_2[4b,6] and TiO_2,[4c] using extended X-ray absorption fine-structure analysis (EXAFS) along with more traditional techniques such as mass spectrometry (MS), transmission electron microscopy (TEM) and temperature programmed reduction (TPR). Gate's and co-worker's more recent studies[7] using the $[Ir(C_2H_4)(–O)_2]$ on dealuminated zeolite Y precatalyst (where $(–O)_2$ indicates the Ir complex is bonded to two surface oxygen atoms from the zeolite support), report that $Ir_{2–4}$ clusters are formed upon exposure to H_2 via EXAFS and infrared spectroscopy.[7] These clusters contain both ethylidyne and di-σ-bonded ethylene ligands and undergo reversible breakup upon exposure to C_2H_4.[7]

Nevertheless, new kinetic monitoring methods for following heterogeneous catalyst formation are needed and would permit a better understanding of the mechanisms of formation of supported heterogeneous catalysts.[8] Such improved kinetic and mechanistic understanding is important in at least three ways:[9] (i) fundamentally, (ii) to gain better control over catalyst syntheses, as well as (iii) practically, since key catalytic properties—including selectivity,[10] activity,[11] lifetime and stability[11]—depend on the catalyst size,[12] surface composition,[13] and structure,[14] which in turn require greater control over heterogeneous-catalyst syntheses.

Especially relevant to our work is Chupas and co-worker's recent, interesting communication monitoring H_2 reduction of H_2PtCl_6 on TiO_2 to form supported $Pt(0)_n$ nanoclusters using in situ time-resolved high-energy X-ray scattering[15] data and the pair distribution function (PDF) method to follow directly the loss of Pt−Cl bonds and the formation of Pt−Pt bonds.[4c] Chupas and co-workers note in their communication that the "kinetics and mechanism of nanoparticle formation and sintering in heterogeneous systems... is... an area that has been largely overlooked, due to the lack of adequate experimental methodology".[4c] Their communication triggered us to report our own, different but related results (vide infra) monitoring H_2PtCl_6 reduction under H_2 to $Pt(0)_n$ on Al_2O_3 or TiO_2. Our results offer an interesting advance in comparison to even that tour de force effort[4c,16] in that we: (i) employ a different, faster, highly convenient and hence much more easily employed, albeit less direct, cyclohexene hydrogenation catalytic reporter reaction monitoring method for following the formation of heterogeneous catalysts;[17] and (ii) study a nontraditional—but more flexible and potentially quite interesting—system where solvent and ligands are present during the supported-catalyst formation. This added flexibility in the supported nanoparticle syntheses[18] offers possible greater control en route to size,[19] shape[20] or composition control over the resultant supported nanoparticles since nucleation and growth can now happen in solution as well as on the support and in the presence of soluble ligands or other additives. In addition, as detailed in what follows our results have allowed us: (iii) to examine quickly a broad range of conditions that uncover H_2 gas-to-solution mass transfer limitations (hereafter MTL) and other issues in the H_2PtCl_6/TiO_2 system (*vide infra*); (iv) to provide product and kinetic evidence consistent with the Finke−Watzky (hereafter F−W) 2-step mechanism of nanocluster formation, and hence our results allow us (v) to tap into the broadest studies and presently best understood solution–based mechanism of transition-metal particle formation and its more than 8 insights for synthesis.[17,21] That repository of kinetic and mechanistic insights include a recent nanoparticle size vs formation time equation that allows size to be controlled as a function of the nucleation (k_1) and growth (k_2) rate constants and the starting concentration of precatalyst, $[A]_0$.[19]

The results reported herein also bear on an interesting 2005 communication from Newton[22] and co-workers, as well as Weaver and co-workers' related studies,[23] monitoring the

(6) Che, M.; Cheng, Z. X.; Louis, C. *J. Am. Chem. Soc.* **1995**, *117*, 2008–2018.
(7) Uzun, A.; Gates, B. C. *Angew. Chem., Int. Ed.* **2008**, *47*, 9245–9248.
(8) We have complied a table of the main prior kinetic and mechanistic studies of heterogeneous catalyst formation, and will report that in due course along with our other, in-progress studies. As stated in the main text a few of the conclusions from compiling that table are (a) additional or improved experimental techniques for following heterogeneous catalyst formation are needed, and (b) more in depth kinetic and mechanistic studies, including the balanced stoichiometry of the catalytst formation reaction, will be required en route to a better, mechanism-based understanding of how to control the syntheses of heterogeneous catalysts.
(9) For these reasons, the present research falls under one of DOE's current Grand Challenges in catalysis, namely the design and controlled synthesis of catalytic structures at the molecular and nanometer level, see: Basic Research Needs: Catalysis for Energy; PNNL-17214; Office of Basic Energy Sciences, U.S. Department of Energy; 2007 (http://www.sc.doe.gov/bes/reports/list.html).
(10) Somorjai, G. A.; Borodko, Y. G. *Catal. Lett.* **2001**, *76*, 1–5.
(11) Ma, Z. ; Zaera, F. In *Encyclopedia of Inorganic Chemsitry*, 2nd ed.; King, B. R., Ed.; John Wiley & Sons Ltd: West Sussex, 2005; Vol. 3, pp 1768−1784.
(12) Che, M.; Bennett, C. O. *Adv. Catal.* **1989**, *36*, 55–172.
(13) (a) Sajkowski, D. J.; Boudart, M. *Catal. Rev.-Sci. Eng.* **1987**, *29*, 325–360. (b) Bond, G. C. *Acc. Chem. Res.* **1993**, *26*, 490–495. (c) Oh, H.-S.; Yang, J. H.; Costello, C. K.; Wang, Y. M.; Bare, S. R.; Kung, H. H.; Kung, M. C. *J. Catal.* **2002**, *210*, 375–386. (d) Tiep, L. V.; Bureau-Tardy, M.; Bulgi, G.; Djega-Maridassou, G.; Che, M.; Bond, G. C. *J. Catal.* **1986**, *99*, 449–460.
(14) Somorjai, G. A. *Catal. Lett.* **1990**, *7*, 169–182.
(15) (a) Billinge, S. J. L.; Kanatzzidis, M. G. *Chem. Commun.* **2004**, 749–760, references therein. (b) Billinge, S. J. L.; Foley, H. C.; Kantazidis, M. G.; Petkov, V.; Thorpe, M. F. *Structure of Nanocrystals*, available online at http://nirt.pa.msu.edu/ (accessed July 2008).
(16) The powerful, direct, high-energy X-ray scattering and pair distribution function (PDF) analysis methods have the large advantage of directly monitoring the loss of Pt–Cl bonds and the formation of Pt–Pt bonds.[4c] The primary disadvantage of these methods is that they are time and effort intensive, and thus relatively slow, with it possible to take even 1−2 years to analyze significant results. Hence, there is a pressing need to prescreen systems and then subject only the most interesting systems to those more direct and powerful, but also more expensive and slower, methods. Important in this regard is that advantages (fast; easy; cheap) and disadvantages (indirect) of the present, fast reporter reaction kinetic method are precisely the opposite of the high-energy X-ray scattering and pair distribution function (PDF) analysis methods (slower and expensive, but direct). Hence, the two methods are highly complimentary. For this reason, a collaboration with the Chupas team has been established in which the general plan is to screen systems with the fast kinetic methods reported herein and then subject the most interesting and important systems to the X-ray scattering methods.
(17) Watzky, M. A.; Finke, R. G. *J. Am. Chem. Soc.* **1997**, *119*, 10382–10400.
(18) (a) Aiken, J. D., III; Finke, R. G. *J. Mol. Catal. A: Chemical* **1999**, *145*, 1–44. (b) Roucoux, A.; Schulz, J.; Patin, H. *Chem. Rev.* **2002**, *102*, 3757–3778.
(19) Watzky, M. A.; Finney, E. E.; Finke, R. G. *J. Am. Chem. Soc.* **2008**, *130*, 11959–11969.
(20) (a) Wang, T.; Lee, C.; Schmidt, L. D. *Surf. Sci.* **1985**, *163*, 181–197. (b) Ahmadi, T. S.; Wang, Z. L.; Green, T. C.; Henglein, A.; El-Sayed, M. A. *Science* **1996**, *272*, 1924–1926. (c) Tao, A. R.; Habas, S.; Yang, P. *Small* **2008**, *4*, 310–325.
(21) (a) Watzky, M. A.; Finke, R. G. *Chem. Mater.* **1997**, *12*, 3083–3095. (b) Aiken, J. D., III; Finke, R. G. *J. Am. Chem. Soc.* **1998**, *120*, 9545–9554. (c) Widegren, J. A.; Aiken, J. D., III; Özkar, S.; Finke, R. G. *Chem. Mater.* **2001**, *13*, 312–324. (d) Hornstein, B. J.; Finke, R. G. *Chem. Mater.* **2004**, *16*, 139–150. See also: Hornstein, B. J.; Finke, R. G. *Chem. Mater.* **2004**, *16*, 3972. (e) Besson, C.; Finney, E. E.; Finke, R. G. *J. Am. Chem. Soc.* **2005**, *127*, 8179–8184. (f) Besson, C.; Finney, E. E.; Finke, R. G. *Chem. Mater.* **2005**, *17*, 4925–4938. (g) Finney, E. E.; Finke, R. G. *Chem. Mater.* **2008**, *20*, 1956–1970.

reduction of a solid 5-wt% Rh_2O_3/γ-Al_2O_3 precatalyst under H_2 gas as a function of temperature. Specifically, we show that the sigmoidal, gas−solid reduction curves reported by Weaver and co-workers can be fit by the F−W 2-step kinetic model (the curves of Newton are more complex and will be analyzed in detail separately). We also show that several literature data sets for the gas−solid reduction of $(CuO)_n$ by H_2 are also well fit by the F−W 2-step model. Those findings—ones summarized in the Supporting Information since the main focus of the present work is $Pt(0)_n$ catalyst formation on Al_2O_3 and TiO_2 and not $Rh(0)_n$—nevertheless still: (a) offer additional support for the greater generality of the F−W kinetic model for the formation of supported catalysts, and (b) providing deconvoluted nucleation (k_1) and growth ($k_2' = k_2[A]_o$) rate constants for those literature systems for the first time. Noteworthy here is that Newton also comments that "the paucity of such detailed kinetic measurements on (the formation of) real, highly dispersed supported catalysts bears testament to their difficulty".[22]

Experimental Section

Materials. All solvents and compounds used were stored in the drybox prior to use. Anhydrous ethanol (Aldrich, 99.5%, 200 proof) packed under nitrogen, ethyl acetate (Aldrich, 99.8%), cyclohexane (99.5%, anhydrous) and chloroplatinic acid hexahydrate (Aldrich, ≥37.5% Pt) were used as received. Cyclohexene (Aldrich, 99%) was freshly distilled over Na metal and under nitrogen. Acidic activated γ-Al_2O_3 (Aldrich), with a surface area of 155 m^2/g was dried at 160 °C in air for 24 h. A mixture of rutile and anatase TiO_2 (Aldrich), with a BET surface area of <100 nm was dried at 160 °C in air for 24 h. Nanopure 18 MΩ-cm H_2O was used from an in house purification system. H_2 gas purchased from General Air (>99.5% purity) was passed through O_2 and H_2O scavenging traps (Trigon Technologies) before use.

Analytical Instrumentation and Procedures. Unless otherwise reported all reaction solutions were prepared under O_2 and moisture free conditions in a Vacuum Atmospheres N_2 filled drybox. The O_2 level (≤5 ppm) is continuously monitored by a Vacuum Atmospheres O_2 sensor. $pH_{apparent}$ measurements were conducted on a Corning pH meter 125 and with a Beckman (511050) dry, gel-filled electrode. (We denote $pH_{apparent}$ since the electrode was used, with calibration, in primarily EtOH but with some H_2O as well as cyclohexene present, vide infra.) TEM analysis was conducted at Clemson University with the expert assistance of JoAn Hudson and her staff. Dark field TEM analysis was done using a Hitachi HD-2000 microscope and bright field TEM analysis was done using both a Hitachi HD-2000 and Hitachi H7600T microscope. EDX analysis was performed on a Hitachi HD-2000 microscope.

Hydrogenation Apparatus and Data Handling. Hydrogenation experiments for monitoring the H_2 reduction of H_2PtCl_6 on Al_2O_3 or TiO_2 to $Pt(0)_n$ on Al_2O_3 or TiO_2 were carried out in a previously described[17,24,25] apparatus to monitor continuously H_2 pressure loss. The apparatus consists of a Fisher-Porter (FP) bottle modified with Swagelock TFE-sealed Quick-Connects to both a H_2 line and an Omega PX621 pressure transducer. The pressure transducer is interfaced to a PC through an Omega D1131 5V A/D converter with a RS-232 connection. Pressure uptake data were collected using LabView 7.1. The hydrogen uptake curves were converted to cyclohexene curves using the previously established 1:1 H_2/cyclohexene stoichiometry.[17,21,26] The data is also corrected for the EtOH solvent-vapor pressure using the previously established protocol.[26] Specifically one can either measure the EtOH vapor pressure independently and subtract that curve (point-by-point) from the raw H_2 uptake data during the cyclohexene reporter reaction, or one can simply back extrapolate the experimental vapor pressure rise (seen in the induction period of the reaction).[26] Both methods yield the same k_1 and k_2 rate constants within a ±15% error. (The k_2 values are corrected by the 2600:1 cyclohexene/H_2PtCl_6 stoichiometry factor as required and as previously done.[21]) Reactions were run at a constant temperature by immersing the FP bottle in a 500 mL jacketed reaction flask containing dimethyl silicon fluid (Thomas Scientific), which was regulated by a thermostatted recirculating water bath (VWR).

Pre-Catalyst Preparation: H_2PtCl_6/γ-Al_2O_3 and H_2PtCl_6/TiO_2. Note that for what follows and throughout this paper, we use wt% defined as wt% = [wt($H_2PtCl_6 \cdot 6H_2O$)/((wt $H_2PtCl_6 \cdot 6H_2O$) + (wt-Al_2O_3))] × 100 and since that is what we experimental measure out and, hence, know. Therefore, our wt% values are different than the more common convention in heterogeneous catalysis of the wt% being the wt of the metal only (e.g., the wt of just Ir in the present case) divided by the total weight (as defined above), all × 100 to convert it into a percentage.

All of the precatalysts were prepared in the drybox using preselected H_2PtCl_6/support weight-to-weight ratios. For example, a 2.0% weight-to-weight H_2PtCl_6/γ-Al_2O_3 sample was prepared by adding 1.0 g Al_2O_3 to 20 mg H_2PtCl_6 (or TiO_2), corresponding to a 1.96-wt% sample, by the following procedure. The appropriate amount of H_2PtCl_6 was weighed out in a 20 mL scintillation vial. A new 5/8 in. × 5/16 in. Teflon-coated octagon shaped stir bar was added to the vial and the solid was dissolved in 15 mL of ethyl acetate. The appropriate amount of solid oxide (e.g., 1.0 g of Al_2O_3 for the 2 wt% Pt catalyst) was added by pouring the metal oxide into the vial (i.e., this order of addition is deliberate, along with an equilibration time that is important, vide infra) and the solution was stirred for 24 h to equilibrate the H_2PtCl_6 with the solid oxide and the solution. After the 24 h period the reaction was taken to dryness in a drybox by placing the sample under vacuum for 8 h at room temperature. The resulting supported precatalysts were stored in the drybox.

Formation of the Active Catalyst: Standard Conditions Reaction. In the drybox 0.05 g of the appropriate H_2PtCl_6/support catalyst precursor was weighed out into a 2 dram scintillation vial. Subsequently, 2.5 mL of ethanol and 0.5 mL of cyclohexene were added via gastight syringes to the 20 dram scintillation vial. A 5/8 in. × 5/16 in. Teflon-coated octagon shaped stir bar was added, the vial was capped and the solution was stirred for 2 h (in catalyst batch #1) and for 7 h (in catalyst batch #2) in the drybox. Catalyst batch #1 and #2 are two different (separately synthesized) batches of the 1.96-wt% H_2PtCl_6/Al_2O_3 precatalyst. The kinetics of the nanocluster formation were reproducible to the average k_1 and k_2 values reported in the main text after these equilibration periods (i.e., control reactions with longer stirring times did not change the kinetics). The solution was then transferred via a disposable polyethylene pipet into a new borosilicate culture tube (22 × 175 mm) with a new 5/8 in. × 5/16 in. Teflon-coated octagon shaped stir bar. The culture tube was sealed in the FP bottle, removed from the drybox, and attached to the H_2 line. The sealed, H_2-line attached FP bottle was placed into the temperature regulated water bath set at 22.0 ± 0.1 °C. The previously developed standard conditions purge cycle[17,27] was used to initiate the reaction, a series of H_2-flushing cycles in which the FP bottle is purged with H_2 every 15 s until 3 min and 30 s have passed (a total of 14 purges). The stir plate was started at 600 rpm, and the H_2 pressure was then set to 40 psig with the data recording started at four minutes after the purge cycle began (i.e., by definition $t = 0$ for the kinetics).

(22) Newton, M. A.; Fiddy, S. G.; Guilera, G.; Jyoti, B.; Evans, J. *Chem. Commun.* **2005**, 118–120.
(23) Williams, C. T.; Chen, E. K.-Y.; Takoudis, C. G.; Weaver, M. J. *J. Phys. Chem. B* **1998**, *102*, 4785–4794.
(24) Lin, Y.; Finke, R. G. *J. Am. Chem. Soc.* **1994**, *116*, 8335–8353.
(25) Aiken, J. D., III; Finke, R. G. *Chem. Mater.* **1999**, *11*, 1035–1047.
(26) Widegren, J. A.; Aiken, J. D., III; Ozkar, S.; Finke, R. G. *Chem. Mater.* **2001**, *13*, 312–324.
(27) Lin, Y.; Finke, R. G. *Inorg. Chem.* **1994**, *33*, 4891–4910.

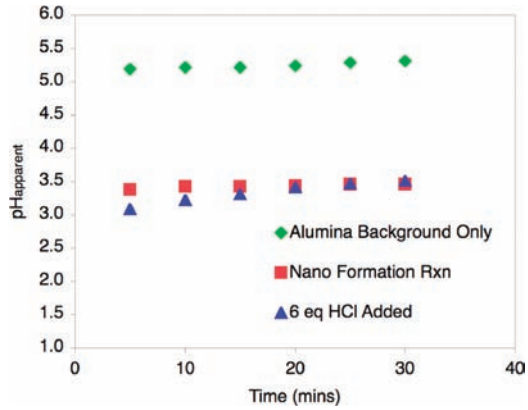

Figure 1. $pH_{apparent}$ measurements confirm the overall nanocluster formation stoichiometry (to within ± 0.1 pH units or ± 20%) for the H_2PtCl_6/Al_2O_3 system shown in Scheme 1.

Scheme 1. Stoichiometry for the H_2PtCl_6/Al_2O_3 Nanocluster System and Cyclohexene Reporter Reaction Studied Herein

Nanocluster Formation Reaction

$$H_2PtCl_6/Al_2O_3 + 2\ H_2 \xrightarrow[40\ psig\ H_2]{EtOH,\ 22^oC} 1/n\ Pt(0)_n/Al_2O_3 + 6\ HCl$$

Cyclohexene Reporter Reaction

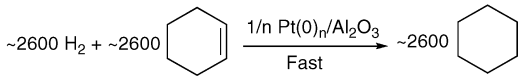

Determination of the Reaction Stoichiometry: $pH_{apparent}$ Measurements. The reaction stoichiometry was determined by measuring the $pH_{apparent}$ of the reaction solution in comparison to a standard solution containing the expected 6 equiv of authentic HCl. First, a Standard Conditions supported nanocluster formation reaction was performed (vide supra). After the reaction was complete, H_2 from the FP bottle was vented and then the FP bottle was brought into the drybox. Next, 5.5 mL of EtOH was added to the reaction mixture and the sample was brought out of the drybox, where 0.5 mL of nanopure H_2O was also added to the solution. The $pH_{apparent}$ was then measured (i.e., the pH in the nanocluster formation solution which also contains EtOH, cyclohexane and added H_2O). Measurements of the $pH_{apparent}$ were also made on (i) a background solution containing 0.05 g Al_2O_3, 8.0 mL EtOH, 0.5 mL cyclohexane and 0.5 mL H_2O ("Alumina Background Control", Figure 1) and, importantly, on (ii) a standard consisting of 0.05 g Al_2O_3, 8.0 mL EtOH, 0.5 mL cyclohexane and 0.5 mL of H_2O containg 6.0 equivalents of HCl ("6 eq HCl added" control, Figure 1), 6 equiv of HCl being the precise amount of acid expected to be generated in the nanocluster formation reaction. The results of these three $pH_{apparent}$ measurements are shown in Figure 1.

Preparation of TEM Grids. Following the preparation of a Standard Conditions supported nanocluster formation reaction, and approximately 2 h after the complete hydrogenation of cyclohexene (as monitored by the H_2 loss curve slowing to effectively zero), the FP bottle was transferred into the drybox. A 300 mesh, Formvar coated SiO_2 TEM grid was dipped in the sample for approximately 5 s and then allowed to dry. The grid was placed in a 2-dram vial, wax sealed and placed in a 20 mL scintillation vial. The TEM grids were sent to JoAn Hudson and her staff at the University of Clemson for TEM analysis.

Results and Discussion

H_2PtCl_6 on Al_2O_3: Precatalyst Synthesis and the Experimental Apparatus. To start, a H_2PtCl_6/Al_2O_3 precatalyst (1.96-wt%) was prepared in a drybox by the addition of Al_2O_3 to a H_2PtCl_6 ethyl acetate solution followed by vacuum drying and as described in the Experimental section. The H_2PtCl_6/Al_2O_3 was then placed in EtOH with ~2600 equivalents of cyclohexene (per equiv of Pt), the mixture sealed in a FP bottle equipped with swage lock quick connects, removed from the drybox, placed in a temperature-regulated water bath, attached to a O_2 and H_2O scrubbed H_2 line, interfaced to a pressure transducer (±0.01 psig) and computer, and stirred at 600 rpms. This now well-described apparatus[17,21,24−27] allows reduction of the H_2PtCl_6/Al_2O_3 precatalyst by H_2 while in contact with ethanol solvent and an olefin (cyclohexene, that is reduced to cyclohexane), Scheme 1, top reaction. This convenient experimental setup also permits the simultaneous, real-time monitoring of the H_2 pressure loss as a means to follow the nanocluster formation kinetics via the also well-established cyclohexene reporter reaction method,[17,21,24−27] Scheme 1, the bottom reaction. Noteworthy here is the contrast of the above (albeit not unprecedented[28]) system with its solid H_2PtCl_6/Al_2O_3 precatalyst in contact with solvent and any other additives such as the olefin cyclohexene, vs traditional heterogeneous catalyst formation systems and their typical H_2 gas−solid reaction.[3]

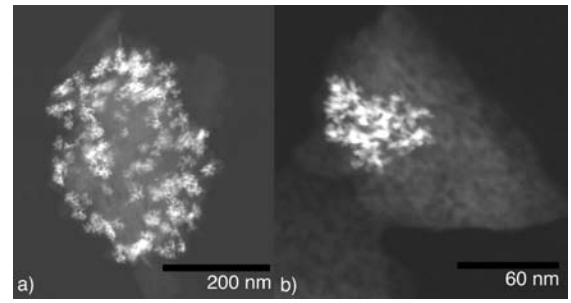

Figure 2. (a) Overall morphology (vs a 200 nm scale bar) of the resultant $Pt(0)_n/Al_2O_3$ catalyst. (b) Expanded image (60 nm scale bar) suggesting that at least some of the observed large clusters in (a) may be formed from agglomerated smaller nanoclusters. Such 2-D images of 3-D supported particles can, of course, misrepresent apparently agglomerated particles as what can actually be individual particles stacked perpendicular to the grid.

H_2PtCl_6 on Al_2O_3: The Reaction Stoichiometry and Product Characterization. A firm knowledge of the products and the balanced reaction stoichiometry is the first rule of reliable mechanistic studies; hence, this is where we began our studies and even though balanced reactions are typically less readily obtained for heterogeneous catalyst formation reactions. Specifically, the stoichiometry in the top of Scheme 1 was confirmed by measuring the H^+ produced (i.e., the $pH_{apparent}$ *vide infra*) and showing it matches (±20%, *vide infra*) a control experiment in which the expected 6 equivalents of HCl was added to the identical volume of a EtOH/cyclohexane solution also containing the same amount of Al_2O_3, Figure 1. Back calculating out the number of moles of H^+ in solution over the 6 data points in Figure 1 for the two, nonbackground samples confirms that the expected 6 equivalents of H^+ are formed (to within ±0.1 pH unit or ±20%). In short, the observed $pH_{apparent}$ and its overlap with the standard where 6 equivalents of authentic HCl is added

(28) (a) De Jong, K. P.; Geus, J. W. *Appl. Catal.* **1982**, *4*, 41–51. (b) Bond, G. C.; Rawle, A. F. *J. Mol. Catal. A: Chem.* **1996**, *109*, 261–271. (c) Sales, E. A.; Benhamida, B.; Caizergues, V.; Lagier, J.-P.; Fiévet, F.; Bozon-Verduraz, F. *Appl. Catal., A* **1998**, *172*, 273–283. (d) Bonet, F.; Grugeon, S.; Urbina, R. H.; Tekaia-Elhsissen, K.; Tarascon, J.-M. *Solid State Sci.* **2002**, *4*, 665–670. (e) Zawadzki, M.; Okal, J. *Mater. Res. Bull.* **2008**, *43*, 3111–3121. (f) Boutros, M.; Denicourt-Nowicki, A.; Roucoux, A.; Gengembre, L.; Beaunier, P.; Gédéon, A.; Launay, F. *Chem. Commun.* **2008**, 2920–2922.

Scheme 2. Illustration of the Cyclohexene Reporter Reaction in which A is the Metal Precursor Complex (H_2PtCl_6 in the Presence of Al_2O_3) and B is Pt(0) on the Growing Nanocluster Surface

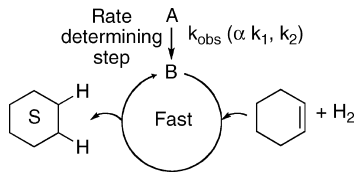

confirms the anticipated HCl formation stoichiometry and is fully consistent with the reaction stoichiometry shown in Scheme 1.

The metal product obtained at the end of the nanocluster formation reaction is visible as a dark gray solid. Dark-field TEM images, Figure 2, and the EDX results shown in the Supporting Information (Figures SI 4 and 5) confirm the formation of 5−10 nm $Pt(0)_n$ nanoclusters supported on the Al_2O_3, particles that more than suffice for the present focus on their kinetics and mechanism of formation.

A control experiment in which the Al_2O_3 is omitted and 0.63 mM H_2PtCl_6 in EtOH and with 1.65 M cyclohexene is run in solution under otherwise identical conditions (e.g., 40 psig H_2) shows different products (bulk metal and a colorless solution devoid, therefore, of significant amounts of H_2PtCl_6). Different kinetics are seen as well (Figure S6 of the Supporting Information) vs the sigmoidal ones seen in the next section for the Al_2O_3 containing system. This control shows that the Al_2O_3 support is as expected an essential part of the present system, without which the (supported) nanoparticles are not formed.

H_2PtCl_6 on Al_2O_3: Catalyst Formation Kinetic Studies. The formation kinetics of the supported $Pt(0)_n/Al_2O_3$ catalyst were obtained using cyclohexene hydrogenation as a precedented reporter reaction,[17,21,24−27] Scheme 2, in which A is the added precursor complex (H_2PtCl_6/Al_2O_3, or its Cl^- dissociated/solvated forms)[29,30] and B is the growing $Pt(0)_n$ nanocluster surface. It is known that the cyclohexene hydrogenation reaction will accurately report on and amplifies the amount of $Pt(0)_n$ nanocluster hydrogenation catalyst, B, present:[17,21,25,26] (i) if there is no H_2 gas-to-solution mass transfer limitations[21b] (MTL), and (ii) when the rate of reduction of cyclohexene to cyclohexane is fast in comparison to the rate of nanocluster formation, k_{obs},[17,21] Scheme 2. The necessary stirring rate dependence plots (Figure S1, Supporting Information) reveal that H_2 gas-to-solution MTL effects are negligible; in addition, [cyclohexene] dependence plots (Figure S2, Supporting Information) approach zero-order in [cyclohexene] as was done before[17] to ensure that the cyclohexene hydrogenation reporter reaction is fast relative to the rate of the (slower) nanocluster formation k_1 and k_2 steps (vide infra). In short, these controls along with prior precedent[17] ensure that the nanocluster formation kinetics are being faithfully monitored.

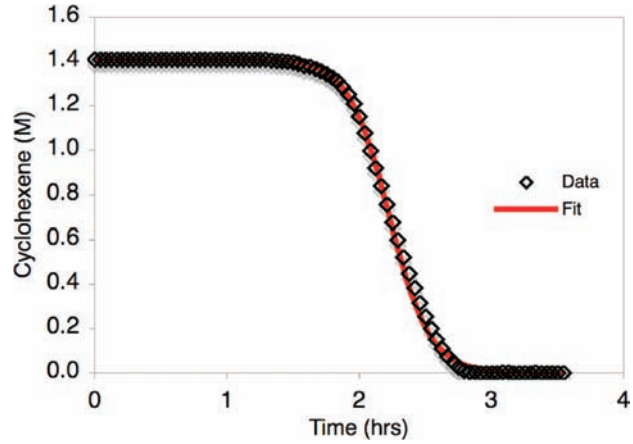

Figure 3. Reproducible kinetics associated with the formation of $Pt(0)_n/Al_2O_3$ and the corresponding excellent fits ($R^2 = 0.9996$) to the F−W 2-step kinetic model of nucleation plus autocatalytic surface growth, Scheme 3.

Scheme 3. F−W 2-Step Mechanism and Its Implied More Detailed Steps (Right) for the 1.96-wt% H_2PtCl_6/Al_2O_3 Precatalyst (A) System En Route to the Supported $Pt(0)_n$ Nanoclusters (B)

$$A \xrightarrow{k_1} B \qquad n\,Pt^{IV} \xrightarrow{H_2} Pt(0)_n$$

$$A + B \xrightarrow{k_2} 2B \qquad Pt^{IV} + Pt(0)_n \xrightarrow{H_2} Pt(0)_{n+1}$$

Experimentally, post monitoring the H_2 uptake with a high-precision (±0.01 psig) pressure transducer it is most convenient to convert and represent the data as cyclohexene consumption, Figure 3, using the known 1:1 H_2/cyclohexene stoichiometry.[17,21] The beauty of this fast, efficient kinetic method[17,21] is that it provides hundreds to thousands (if desired) of high precision data points for the catalyst formation, more—as well as more precise—data than obtainable by other present methods, to our knowledge.

The resultant kinetics for the formation of $Pt(0)_n$ nanoclusters on Al_2O_3, Figure 3, are interesting. Specifically, sigmoidal kinetics for the $Pt(0)_n/Al_2O_3$ formation reaction are seen and closely fit by the F−W 2-step, nucleation and autocatalytic growth mechanism of nanocluster formation, Scheme 3, first

(29) An important topic, one that will require its own extensive studies to unravel, is the nature of the precise Pt speciation when H_2PtCl_6 is placed on supports such as Al_2O_3 as well as the kinetic contribution of each species to $Pt(0)_n$ formation. There is literature on the speciation of H_2PtCl_6 in aqueous solutions as well as in the presence of Al_2O_3.[30] However, no real consensus exists at present on either the exact species present in solution or on the Al_2O_3 support. The literature is clear that $[PtCl_6]^{2-}$, aquo species such as $[PtCl_5(H_2O)]^-$, aquahydroxo species such as $[PtCl_4(OH)(H_2O)]^-$ along with many others exist in aqueous solutions, and that such speciation is highly pH dependent. The exact interaction of the species formed from aqueous H_2PtCl_6 with the Al_2O_3 support is also a controversial subject.[30b,c] Regalbuto[30a] suggests that when fresh H_2PtCl_6 solutions are prepared the major species present in solution is $[PtCl_3(H_2O)_3]^+$, and it is repelled from the protonated $[Al_2O_3]^+$ surface at low pH. However the major species present in aged H_2PtCl_6 solutions in a mid-pH of 5−9 (as defined by those authors[30b]) is $[PtCl_2(OH)_2(H_2O)_2]^0$, and this species should more readily interact with the Al_2O_3 support. In the present studies, we use ethyl acetate for the H_2PtCl_6 impregnation step in a deliberate attempt to minimize any subsequent speciation and to emphasize support of the neutral, parent complex. However, during our kinetic runs the H_2PtCl_6/Al_2O_3 is in contact with the EtOH and cyclohexene solution, so that additional speciation is possible if not probable. Experimentally, we know that the kinetics of H_2PtCl_6 reduction in EtOH plus cyclohexene solutions (but without Al_2O_3 present) are different than the kinetics when Al_2O_3 is present; hence, the support must be playing a role in the observed catalyst formation kinetics. The good news here is that the ability of the catalytic reporter reaction method to rapidly monitor the kinetics of nanoparticle formation will allow the needed survey of a range of supports, metal, and other conditions. Such experiments should yield insights into the Pt speciation and into many other unanswered questions regarding how to best prepare superior supported-nanoparticle heterogeneous catalysts.

(30) (a) Spieker, W. A.; Liu, J.; Miller, J. T.; Kropf, A. J.; Regalbuto, J. R. *Appl. Catal., A* **2002**, *232*, 219–235. (b) Spieker, W. A.; Liu, J.; Miller, J. T.; Kropf, A. J.; Regalbuto, J. R. *Appl. Catal., A* **2003**, *243*, 53–66. (c) Shelimov, B. N.; Lambert, J.-F.; Che, M.; Didillon, B. *J. Mol. Catal. A: Chem.* **2000**, *158*, 91–99. (d) Mang, T.; Breitscheidel, B.; Polanek, P.; Knözinger, H. *Appl. Catal., A* **1993**, *106*, 239–258. (e) Brunelle, J. P. *Pure Appl. Chem.* **1978**, *50*, 1211–1229.

worked out in 1997 for soluble nanocluster formation.[17] The average rate constants (from 8 independent kinetic runs) for nucleation ($k_1 \approx 10^{-5.5(7)}$ h^{-1}) and autocatalytic growth ($k_2 = 1.2(2) \times 10^4$ h^{-1} M^{-1}) from the Pt(0)$_n$/Al_2O_3 supported nanoclusters are obtained from a nonlinear least-squares fit to the analytic integrated rate equation derived from the 2-step kinetic model (shown in the Supporting Information). Importantly, the observed kinetics are reproducible to the given error bars[31] from batch-to-batch of freshly synthesized H_2PtCl_6/Al_2O_3 precatalyst, so long as one employs a prestirring/pre-equilibration period of ca. 2−7 h at 22 °C in which the H_2PtCl_6 or its Cl^- dissociated/solvated[29,30] forms become equilibrated with the Al_2O_3 support and solution. Shown in the Supporting Information are the different curves that one can obtain if insufficient equilibration times are used, results that readily reveal this important-for-synthesis, pre-equilibration time.

The observed kinetics and excellent fit to the F−W 2-step mechanism[17,21] are on one hand not entirely unexpected,[17,21,32,33] but are still quite significant. For starters, the fit to the 2-step model and the resultant nucleation (k_1) and autocatalytic growth (k_2) rate constants imply that all of ≥8 available insights into soluble nanocluster synthesis and stabilization[17,21] should be applicable, at least in principle, to supported-nanocluster heterogeneous catalysts, insights which include: (i) understanding how to form routinely near-monodisperse (≤ ±15%) size distributions of typically "magic-number sized" (i.e., full shell)[21a] size distributions of supported nanoclusters; (ii) *rational size control* via a recently developed nanocluster size vs time equation in terms of k_1, k_2 and the precatalyst concentration, $[A]_o$,[19] (iii) additional possible size control via olefin or other ligand dependence,[24,27] (iv) rational use of seeded-growth methods including the rational synthesis of all possible geometric isomers of multimetallic "nano-onions"[21a] (v) rational catalyst shape control via ligands capable of attaching to the growing nanocluster faces and thereby preventing autocatalytic surface growth of that facet;[20] (vi) knowledge of the negative effects of, and insights into how to avoid, H_2 gas-to-solution mass-transfer limitations (MTL) in nanocluster syntheses; [21b] (vii) knowledge of what added nanocluster surface ligands can provide additional nanocluster stability if desired;[34] and (viii) the possibility of nanocluster size-dependent surface metal-to-ligand bond energies-and all that preliminary finding implies for catalysis.[21e−g]

Scheme 4. One Possible Mechanism Consistent with the Observed Linear $[H_2PtCl_6/TiO_2]^0$ Kinetics Seen for the Literature Gas-Solid Catalyts Formation System[4c] [a]

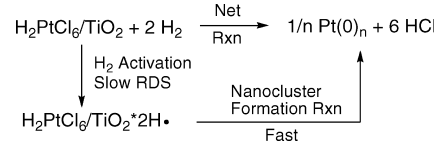

[a] The net reaction is shown on the top of the scheme and on the bottom H_2 activation is postulated as the slow, rate-determining step.

More immediately, however, we were able to apply the insight that the F−W 2-step mechanism fits the 1.96-wt% H_2PtCl_6/Al_2O_3 system, to gain insights about the related, but interestingly different, system of H_2PtCl_6/TiO_2. Those observed differences must mirror the differences in the TiO_2 vs Al_2O_3 supports since that is the only difference between the two systems, vide infra.

H_2PtCl_6 on TiO_2: Catalyst Formation Kinetics. The knowledge that the 2-step F−W mechanism quantitatively accounts for the kinetics of conversion of H_2PtCl_6/Al_2O_3 to Pt(0)$_n$/Al_2O_3 caused us to re-examine—but now under our solution containing system and conditions—the interesting 5-wt% H_2PtCl_6/TiO_2 precatalyst plus H_2 system recently communicated to this journal, but which was examined under the more traditional conditions of reduction via a H_2 gas−solid interface.[4c] Specifically, the recently observed,[4c] intriguing linear loss and implied zero-order dependence on the H_2PtCl_6/TiO_2 precursor, +d[Product]/dt α $[H_2PtCl_6/TiO_2]^0$, in the literature H_2 gas−solid precatalyst system caught our attention. Such a zero-order dependence, $[H_2PtCl_6/TiO_2]^0$, to an end Pt(0)$_n$/TiO_2 product, requires one to write a mechanism not involving H_2PtCl_6 in the rate-determining step. Rate-determining H_2 activation on TiO_2 is about the only rational mechanism one can write, Scheme 4, and assuming facile H• diffusional transfer to the active site where H_2PtCl_6 is reduced.

The implication is that the rate-controlling H_2 activation (and/or or possibly a slow H• transfer) are obscuring the desired kinetics of nanoparticle formation. While the direct monitoring of Pt−Cl loss and Pt−Pt formation is the power of the elegant high-energy X-ray scattering and pair distribution function (PDF) methods reported recently, those methods are relatively slow and expensive[16] so that studies under the chemically interesting conditions where the catalyst formation rate is not zero-order in $[H_2PtCl_6/TiO_2]$ have yet to be reported. Hence, it is of interest to examine the H_2PtCl_6/TiO_2 system by the reporter reaction methods developed herein so that a broader range of conditions can be more quickly examined. It is also of considerable interest to combine the present methods with more direct, powerful X-ray scattering methods.[16]

Intriguingly, under our solution-based conditions and using our catalytic reporter reaction monitoring method, we, too, see linear kinetics for the same 5-wt% H_2PtCl_6 on TiO_2,[4c] even though our system is not the gas−solid system but is in EtOH, 1.65 M cyclohexene, and has these reagents plus H_2 gas initially at 40 psig in contact with the stirred solution, Figure 4. The F−W 2-step mechanism does not fit the experimental data as expected since those data are basically a straight line. The observed zero-order kinetics for the H_2PtCl_6/TiO_2 system, Figure 4, and the implicated H_2 gas-to-solution MTL effects (vide infra), were further supported by the studies summarized in Figure 5, in which the observed H_2 uptake rate vs the Pt-wt% is plotted. Further confirmation of MTL effects for the 5-wt% H_2PtCl_6/TiO_2 system were obtained by the kinetic data in Figure

(31) For the error limits in k_1 ($\sim\pm10^{1.2}$ h^{-1}) and k_2 ($\sim1(3) \times 10^2$ M^{-1} h^{-1}) observed in multiple investigator's hands over a 7+ year period for $P_2W_{15}Nb_3O_{62}^{9-}$ polyoxoanion-stabilized Ir(0)$_{\sim300}$ nanoparticle formation, see p. 10304 of Widegren, J. A.; Bennett, M. A.; Finke, R. G. *J. Am. Chem. Soc.* **2003**, *125*, 10301–10310.

(32) (a) Although the 2-step F−W kinetic model is consistent with all of the present data as well as a considerable body of prior kinetics (more than 700 runs) of nanocluster formation under H_2,[17,21] it needs to be emphasized that the F−W kinetic model is a deliberately minimalistic, "Ockham's razor"-obtained model. As just one example of presently unknown details, the fuller mechanism presumably involves ligated nanocluster, M_a-L_b (M = metal), intermediates as well as possible nanocluster hydride, M_c-H_d, intermediates,[21c,g] since naked M(0) atoms are highly energetic and thus relatively unstable.[17,21c,g] Of interest in this regard is that metal-hydrides have been previously postulated to be the aggregating species in supported catalyst formation.[33] Elsewhere we discuss the limitations of the F−W model, limitations that derive ultimately from its minimalistic nature.[37,38]

(33) (a) Dalla Betta, R. A.; Boudart, M. In *International Congress on Catalysis*, 5th ed.; North-Holland: Palm Beach, FL, 1972; Vol. 5th Annual, pp 1329−1341. (b) Reagan, W. J.; Chester, A. W.; Kerr, G. T. *J. Catal.* **1981**, *69*, 89–100.

(34) Ott, L. S.; Finke, R. G. *Coord. Chem. Rev.* **2007**, *251*, 1075–1110.

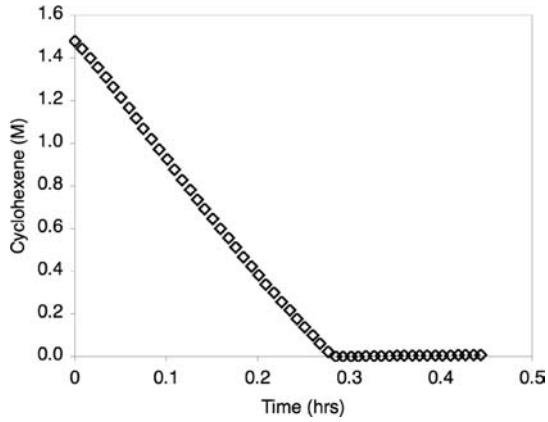

Figure 4. Linear kinetics observed for the 5-wt% H_2PtCl_6/TiO_2 system herein in contact with stirred EtOH and cyclohexene. The curve shows no discernible induction period; hence it is not fit to the F−W 2-step mechanism.

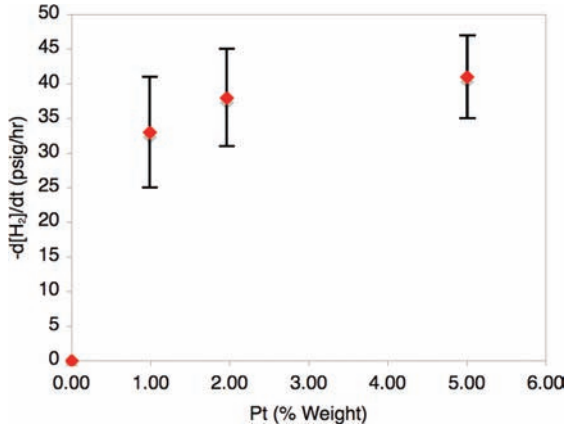

Figure 5. Rate of H_2 loss as a function of the Pt-wt%. The reaction approaches zero-order kinetics, and thus enters a H_2 gas-to-solution MTL regime, even by 2-wt% Pt (with complete MTL by 5-wt% Pt) for H_2PtCl_6/TiO_2 (and in our specific apparatus, stirring conditions, H_2 pressure, solvent, temperature and other conditions that influence MTL).

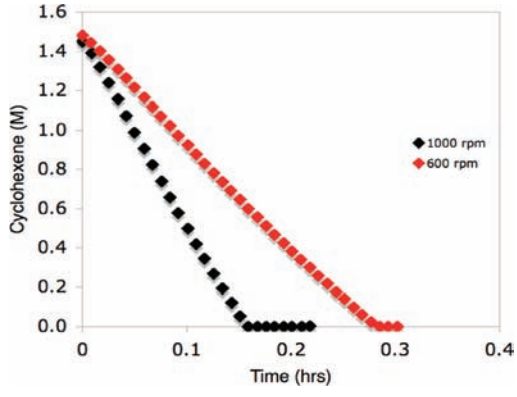

Figure 6. Comparison of the kinetics observed for the 5-wt% H_2PtCl_6/TiO_2 sample stirred at both 600 and 1000 rpms. Note the large increase in the reaction rate at 1000 rpms (66.8 mmols H_2/hr vs 42.2 mmols H_2/hr), indicating H_2 gas-to-solution MTL effects are present in this system.

6, the loss of cyclohexene was measured as a function of stirring speed, 600 rpms and then 1000 rpms, respectively. The figure shows a large increase in the rate of cyclohexene uptake (or H_2 uptake) as a function of increasing stirring speed. Specifically the rate of H_2 uptake (calculated using the method of initial

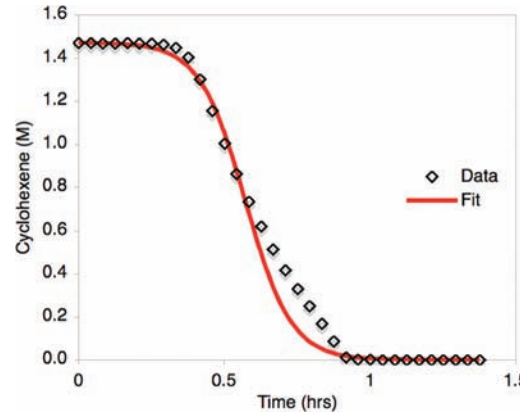

Figure 7. $Pt(0)_n$ on TiO_2 nanocluster formation kinetics for the 0.99-wt% H_2PtCl_6/TiO_2 system. One can see the sigmoidal kinetics-and the reasonable but not great fit to the F−W 2-step mechanism ($R_2 = 0.9964$). The lower catalyst loading conditions reveal the sigmoidal nucleation ($k_1 = 1.8(9) \times 10^{-2}\ h^{-1}$) and autocatalytic growth ($k_2 = 5.0(6) \times 10^4\ h^{-1}\ M^{-1}$) nanoparticle formation kinetics as compared to Figure 4.

rates,[35] and then expressed in Figure 6 as its equivalent cyclohexene loss kinetic data) exhibits a significant dependence on stirring rate, 42.2 psig H_2/hr at 600 rpm vs a 58% higher 66.8 psig H_2/hr at a ca. 66% higher, 1000 rpm stirring rate. Overall, the above data are prima facie evidence consistent with unwanted H_2 gas-to-solution MTL effects in the 5-wt% H_2PtCl_6/TiO_2 system. Such MTL effects of course obscure the desired, underlying nanoparticle formation chemical mechanism.

However and importantly, the above evidence for MTL effects, plus our ability to rapidly screen conditions, allowed us to quickly find lower metal loading conditions (0.99-wt% H_2PtCl_6/TiO_2) *that unmask sigmoidal-type kinetics*, thereby revealing the desired nanocluster formation chemical kinetics. The 0.99-wt% H_2PtCl_6/TiO_2 data, along with the corresponding fit to the F−W nanocluster formation mechanism, is shown in Figure 7. The data and fit in Figure 7 also reveal that even the 0.99-wt% H_2PtCl_6/TiO_2 system still is under some MTL (results which are elaborated on in the SI for the interested reader). However, the sigmoidal features in Figure 7 make it clear the change to a lower catalyst loading is having the anticipated, desired effect of moving away from the chemically uninteresting MTL regime.

The observation that the lower loading 0.99-wt% H_2PtCl_6/TiO_2 still has MTL effects, even though these are minimized for the somewhat higher loading 1.96-wt% H_2PtCl_6/Al_2O_3 precatalyst, is interesting. While not fully understood, this observation of less MTL in the Al_2O_3-supported precatalyst despite it being at nearly 2-times the metal loading: (a) shows the significant effect of the support on the catalytst formation kinetics, and (b) argues for different H_2PtCl_6 speciation on these two supports (with a more active species toward Pt(0) formation on TiO_2)[29] as one of the few, possible explanations that is apparent at present. This observation of the support effect on catalyst formation also makes clear that (c) such support effects are a topic that will merit a range of their own, in-depth studies to achieve a better understanding of such interesting, catalyst-synthesis-relevant, support effects.

The value of the methods reported herein, for rapidly screening kinetics of supported nanoparticle formation under

(35) Wilkins, R. G. *Kinetics and Mechanism of Reactions of Transition Metal Complexes*, 2nd ed.; VCH: New York, 1991.

at least our solution-containing conditions, is noteworthy. In addition, our results already provide an important insight into the synthesis and formation of heterogeneous catalysts, namely the need to avoid MTL effects that are known to lead to broad distributions of nanoclusters.[21b] Exciting here is the collaboration we have initiated with the Argonne group[4c] to use the advantage of each of our separate methods, while minimizing exposure to each method's disadvantages,[16] in further studies of the H_2PtCl_6/TiO_2 and other supported nanocluster catalysts systems. Studies meriting additional scrutiny include the interesting comparison of the gas−solid vs gas-solution-solid based systems and studies of other supports and their effects.

Initial Application of the F−W 2-Step Kinetic Model to Other Heterogeneous Catalyst Formation Systems. Sigmoidal reduction kinetics have also been observed by Weaver and co-workers,[23] for the reduction of Rh_2O_3 thin films followed by surface-enhanced Raman spectroscopy (SERS), as well as by Newton and co-workers,[22] for the H_2 reduction of Rh_2O_3 particles on γ-Al_2O_3 followed by the XANES edge. Sigmoidal curves are also common in the $(CuO)_n$ H_2 gas−solid reduction literature, for example in the reduction $(CuO)_n$ by H_2.[36] However, none of the sigmoidal kinetic curves in those studies were quantitatively fit, testament to the general lack until recently[17,37,38] of kinetic models able to fit the kinetics of such phase-change phenomenon with a chemical-mechanism-based equation.[17,37,38] In for example the 2005 study of the H_2 reduction of Rh_2O_3 particles on γ-Al_2O_3,[22] primarily the post-induction period part of the kinetic curve was analyzed and used to provide apparent activation parameters for the second part of the kinetic curve (that we know from the studies herein is largely the growth phase).

Using the F−W kinetic model, we have fit or attempted to fit the Rh_2O_3[22,23] data as well as the $(CuO)_n$[36] reduction data we mined from the literature. These data, provided in the SI for the interested reader, demonstrate sigmoidal M_xO_y reduction curves for *gas−solid* reactions can be fit in at least 2 of the 3 cases examined by the F−W 2-step mechanism and that k_1 nucleation and, now, k_2' (= $k_2[A]_o$; see the SI) autocatalytic growth rate parameters can be deconvoluted from those fits, previously unreported resutls. The importance of these fits to literature gas−solid heterogeneous catalyst formation kinetic data is they show the broader applicability of the F−W 2-step kinetic model to at least some H_2 gas−solid M_xO_y reduction systems.

Conclusions

In conclusion we have demonstrated: (i) the ability to monitor heterogeneous catalyst formation rapidly and in real time using the fast catalytic reporter reaction method developed previously;[17,21] (ii) that the formation kinetics are well fit by the F−W 2-step mechanism of slow, continuous nucleation followed by fast autocatalytic surface growth first worked out for soluble nanocluster formation;[17] and (iii) that the ≥8 insights available from solution based nanoparticle mechanism of formation studies[17,21] should, therefore, be applicable at least in principle en route to supported nanocluster heterogeneous catalysts with potentially rationally improved size, shape, multimetallic nano-onion and other mechanism-based synthetic control. In addition, we: (iv) have studied a relatively little-investigated, flexible solution-solid heterogeneous catalyst formation system where added ligands, solvent and so on can be employed to gain additional control over the formation of the supported metal particles; and (v) have demonstrated the ability to screen rapidly supported heterogeneous catalyst formation, thereby allowing MTL effects in the H_2PtCl_6/TiO_2 precatalyst systems to be uncovered, in turn allowing lower [catalyst] loading conditions to be used to unmask the desired chemical kinetics and mechanism of nanoparticle formation. Finally, we: (vi) have also shown that the weaknesses and strengths of the catalytic reporter reaction monitoring method are a good match for the, respectively, complimentary strength and weakness of the powerful, direct, high-energy X-ray scattering methods[4c] so that it is of considerable interest to use these two methods (or similar ones) *in tandem*; and (vii) have demonstrated the applicability of the F−W kinetic model to 2 of 3 sets of literature heterogeneous catalyst formation from Rh_2O_3 and $(CuO)_n$ gas−solid reductions, allowing nucleation and growth rate constants to be obtained from those data sets for the first time, results which demonstrate the broader applicability of the F−W kinetic model to at least some other, in those cases H_2 gas, M_xO_y solid, heterogeneous catalyst formation systems.[39]

It is our hope that others will employ the methods and kinetic model presented herein, but while keeping the limitations of the reporter reaction method and the minimalistic F−W model well in mind.[37,38] The results of our own additional studies of the present systems, as well as other metals and a range of different support materials, will be reported in due course.

Acknowledgment. We thank Dr. P. Chupas and co-workers for enlightening discussions of their interesting work.[4c] This work was funded by DOE Grant DE-FG02-03ER15453.

Supporting Information Available: MTL and zero-order cyclohexene plots; EDX; additional 1.96-wt% H_2PtCl_6/Al_2O_3 kinetics; unsupported H_2PtCl_6 reduction kinetics in EtOH, 0.99-wt% H_2PtCl_6/TiO_2 MTL data; and fits to 7 sets of H_2 plus M_xO_y gas−solid catalyst formation kinetic data by the F−W 2-step kinetic model. This material is available free of charge via the Internet at http://pubs.acs.org.

JA808980A

(36) Rodriguez, J. A.; Kim, J. Y.; Hanson, J. C.; Perez, M.; Frenkel, A. I. *Catal. Lett.* **2003**, *85*, 247–254.

(37) Sigmoidal kinetic curves for protein aggregation fit by the F−W 2-step kinetic model, papers that also contain a detailed discussion of the limitations of the F−W kinetic model (see also elsewhere for a general discussion of the limitations of models in science[38]) all types: (a) Morris, A. M.; Watzky, M. A.; Agar, J. N.; Finke, R. G. *Biochemistry* **2008**, *47*, 2413–2427. (b) Watzky, M. A.; Morris, A. M.; Ross, E. D.; Finke, R. G. *Biochemistry* **2008**, *47*, 10790–10800. (c) Morris, A. M.; Finke, R. G. *Biophys. Chem.* **2009**, *140*, 9–15.

(38) "Fitting and Interpreting Transition-Metal Nanocluster Formation and Other Sigmoidal-Appearing Kinetic Data: A More Thorough Testing of Dispersive Kinetics vs Chemical-Mechanism-Based Equations and Treatments" Finney, E. E.; Finke, R. G. *Chem. Mater.*, submitted.

(39) The successful extension of the F-W model to gas solid-reactions is not surprising given that metal thin-film formation have been previously shown to follow the F-W model in at least the one case examined. Widegren, J. A.; Bennett, M. A.; Finke, R. G. *J. Am. Chem. Soc.* **2003**, *125*, 10301–10310.